



RESEARCH LETTER

10.1002/2017GL073625

Key Points:

- The Madden-Julian Oscillation (MJO) modulates monsoon disturbances globally
- Off-equatorial monsoon disturbances peak near MJO low level vorticity maxima
- Equatorial monsoon disturbances peak in MJO low level zonal wind convergence

Correspondence to:

P. Haertel
patrick.haertel@yale.edu

Citation:

Haertel, P., and W. R. Boos (2017), Global association of the Madden-Julian Oscillation with monsoon lows and depressions, *Geophys. Res. Lett.*, *44*, 8065–8074, doi:10.1002/2017GL073625.

Received 12 MAY 2017

Accepted 10 JUL 2017

Accepted article online 12 JUL 2017

Published online 14 AUG 2017

Global association of the Madden-Julian Oscillation with monsoon lows and depressions

Patrick Haertel¹  and William R. Boos¹ 

¹Department of Geology and Geophysics, Yale University, New Haven, Connecticut, USA

Abstract Previous research has revealed that monsoon lows and depressions are modulated on intraseasonal time scales in a few regions, including India, Australia, and the East Pacific. This study examines whether such modulation occurs on a global scale and, in particular, how the Madden-Julian Oscillation (MJO) is associated with changes in synoptic-scale vortices across all monsoon regions. The spatial climatology of monsoon disturbances is largely insensitive to MJO amplitude. However, monsoon disturbance frequency (MDF) varies substantially with MJO phase, with regional perturbations of 25 to 90% of the seasonal mean value across the tropics. In off-equatorial locations, MDF maxima occur in locations where the MJO enhances low level cyclonic vorticity, typically near the western edge of midlevel moisture perturbations. In contrast, equatorial MDF perturbations are in phase with MJO moisture and rainfall anomalies, with maxima in regions with strong low level zonal wind convergence.

1. Introduction

The Madden-Julian Oscillation (MJO) is a planetary-scale tropical weather disturbance with a convective signal that propagates slowly eastward over the Indian and West Pacific Oceans [Madden and Julian, 1971, 1972, 1994; Zhang, 2005]. The MJO's heaviest rainfall is accompanied by a deep moisture anomaly, strong westerly surface winds, and off-equatorial upper tropospheric cyclonic and anticyclonic gyres leading and trailing the precipitation maximum, respectively [Kiladis et al., 2005]. While the MJO's cloudiness primarily propagates eastward in boreal winter, during boreal summer its convective anomalies also move northward near Southeast Asia [Wang and Rui, 1990].

The MJO has many important impacts on weather and climate. First, it has a stronger spectral signal in cloudiness and rainfall than other convectively coupled equatorial waves [Wheeler and Kiladis, 1999]. Second, it modulates tropical cyclones over the Atlantic, Pacific, and Indian Oceans [Liebmann et al., 1994; Maloney and Hartmann, 2000; Bessafi and Wheeler, 2006]. Third, it affects the strength of the Asian, Australian, and North American monsoons [Wu et al., 1999; Lorenz and Hartmann, 2006]. Finally, MJO westerly wind bursts impact the timing and diversity of El Niño events [Fedorov et al., 2015].

Here we focus on the MJO's association with synoptic-scale precipitating vortices in monsoon regions, which are well known over India, where weaker vortices are called lows and stronger vortices are called depressions. Monsoon lows and depressions with similar structures are also prevalent in the Australian summer monsoon and in the West Pacific [Davidson and Holland, 1987; Hurley and Boos, 2015]. There are more monsoon lows and depressions during the convectively active phase of the MJO over both Australia and India than there are during the convectively suppressed phase [Berry et al., 2012; Yasunari, 1981; Chen and Weng, 1999; Goswami et al., 2003; Krishnamurthy and Ajayamohan, 2010]. The MJO also modulates the amplitude, structure, and frequency of synoptic-scale waves in the tropical East Pacific with strong low level to midlevel vorticity signals [Rydbeck and Maloney, 2014, 2015; Crosbie and Serra, 2014]. However, it is difficult to compare the strength and nature of the modulation of synoptic-scale vortices across these regions because of the fundamentally different metrics used in these previous studies. For example, Berry et al. [2012] used reanalyzed potential vorticity on the 315 K isentropic surface to count Australian monsoon lows and depressions, while most studies of Indian monsoon synoptic activity rely on a subjectively analyzed compilation of lows and depressions [Mooley and Shukla, 1987; Sikka, 2006], and studies of the MJO's modulation of East Pacific synoptic-scale waves have used local principal component analyses to construct wave composites [Rydbeck and Maloney, 2014, 2015; Crosbie and Serra, 2014].

Here we relate the global distribution of monsoon lows and depressions to the dominant mode of global intraseasonal variability. We use tracks of monsoon lows and depressions compiled using objective, automated algorithms applied to reanalysis data [Hurley and Boos, 2015], and examine the association of genesis frequency and track density with the widely used real-time, multivariate MJO index of Wheeler and Hendon [2004]. This provides the first global view of the statistical association between intraseasonal variability and synoptic-scale monsoon vortices.

2. Data and Methods

2.1. Monsoon Disturbance Data Set

We use the monsoon low and depression track data set developed by Hurley and Boos [2015], which was created by tracking 850 hPa relative vorticity anomalies in the ERA-Interim reanalysis [Dee et al., 2011] from 1979 to 2012. Storms are classified as “monsoon low,” “monsoon depression,” or “deep depression” based on their surface pressure anomaly and maximum surface wind speed [Hurley and Boos, 2015]. The data set only contains disturbances that originate in the region on the equatorial side of a line drawn 500 km poleward of the 850 hPa temperature maximum. This includes the precipitating monsoon regions of Africa, Asia, Australia, and the tropical Americas, together with the desert regions that lie poleward of these moist monsoon zones. Here we focus on low-pressure systems that have a precipitable water content of at least 53 mm; these moist vortices are precipitating and they have deep-tropospheric wind anomalies [Hurley and Boos, 2015; Ditchek et al., 2016].

There is some overlap between the populations of monsoon disturbances and tropical cyclones, but most monsoon disturbances are not represented in best-track data sets of tropical cyclones. For example, the International Best Track Archive for Climate Stewardship (IBTrACS) contains only 86 tropical cyclone tracks in the Northern Indian Ocean basin during the boreal summer (May–September) months of 1990–2011, while our data set contains 453 monsoon disturbance tracks in the same region for that period. Of the 86 cyclones in IBTrACS, all but seven have a counterpart in the monsoon disturbance data set (i.e., a disturbance that has a similar track). Our data set includes disturbances having weak surface wind speeds that are often excluded from studies of the intraseasonal modulation of tropical cyclones (Liebmann et al., 1994).

2.2. Rainfall

To generate composite rainfall patterns for the MJO, we use data from the Global Precipitation Climatology Project [Huffman et al., 2001] for 1 October 1996 to 31 December 2012, which we average into $5 \times 5^\circ$ bins to better highlight variability on larger spatial scales. While these observations cover a shorter time period than the monsoon disturbance data, comparisons of monsoon disturbance frequency and rainfall perturbations for individual MJO phases (see section 3) yield a consistent picture of where atmospheric convection is enhanced. Moreover, we prefer using rainfall measurements as opposed to data indicative of high cloudiness (outgoing longwave radiation) and thus are willing to accept the more limited historical record of the former.

2.3. Reanalysis

ERA-Interim data for 1979–2012 are used to assess the association of atmospheric variables with monsoon disturbance activity. To isolate the planetary structure of the MJO, we apply a 7–70 day band-pass filter and average data into bins that span 30° of longitude and 10° of latitude. The time- and space-filtered data are then averaged over each MJO phase.

2.4. MJO Index and Compositing Method

To identify the amplitude and phase of the MJO, we use the real-time multivariate MJO (RMM) index of Wheeler and Hendon [2004], which was downloaded from the Australian Bureau of Meteorology and is currently available from <http://www.bom.gov.au/climate/mjo> under the heading “RMM data.” This index is available for the entire 34 year duration of the monsoon-disturbance data set. To create composite MJO perturbations, we average data for each phase of the MJO for all times when MJO amplitude is greater than 1.

3. Relationship Between MJO and Monsoon Disturbance Activity

3.1. MJO Amplitude and the Spatial Climatology of Monsoon Disturbances

We first consider how MJO amplitude affects the spatial distribution of monsoon disturbances over seasonal time scales. Figures 1a and 1b show meridionally integrated genesis frequencies for each category of

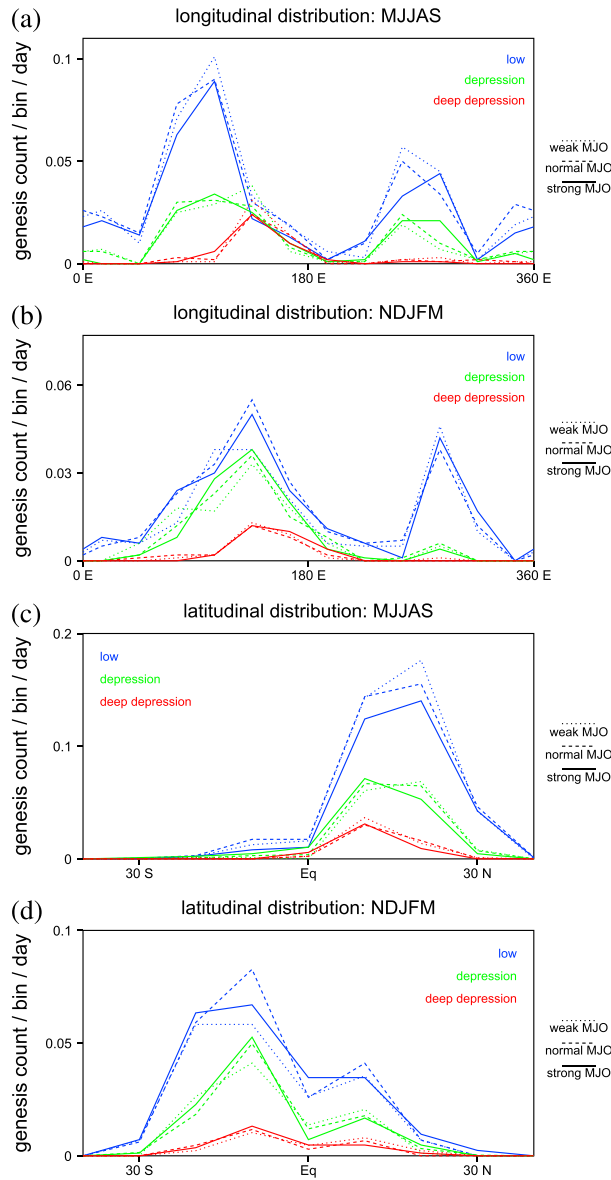


Figure 1. Dependence of monsoon disturbance genesis on MJO amplitude. Longitudinal distribution for (a) May–September and (b) November–March. Latitudinal distribution for (c) May–September and (d) November–March. Bins span 30° longitude or 10° latitude.

monsoon disturbance for winter and summer seasons, stratified by longitude and MJO amplitude. We consider frequencies for days when the MJO amplitude is greater than one standard deviation above its seasonal mean value (solid lines), within one standard deviation of the seasonal mean value (dashed lines), and more than one standard deviation below the seasonal mean value (dotted lines). Overall, the longitudinal distribution of genesis frequency is surprisingly insensitive to MJO amplitude. For both boreal winter and summer seasons, and for most longitudes, roughly the same number of monsoon disturbances of each category develop in each longitudinal bin when MJO amplitude is high, near normal, and low. One exception is for the eastern Pacific in the boreal summer (Figure 1a), for which there are fewer monsoon lows when the MJO amplitude is high, and the peaks for both lows and depression shift eastward in this case. We also constructed similar plots showing how the latitudinal distribution of monsoon disturbances varies with MJO amplitude (Figures 1c and 1d), which provide the same general result: in most latitudes there are roughly the same number of lows, depressions, and deep depressions for a range of MJO amplitudes. The most notable exception in this case is in the boreal summer in the Northern Hemisphere, where the genesis frequency of monsoon lows decreases with increasing MJO amplitude (Figure 1c, blue curves). We also examined how global counts of monsoon disturbances vary with MJO amplitude (not shown) and found little change for each category of disturbance. We conclude that variations in MJO amplitude cause little cumulative change to monsoon disturbance frequency over seasonal time scales and only minor shifts in the spatial climatology.

global counts of monsoon disturbances vary with MJO amplitude (not shown) and found little change for each category of disturbance. We conclude that variations in MJO amplitude cause little cumulative change to monsoon disturbance frequency over seasonal time scales and only minor shifts in the spatial climatology.

3.2. MJO Phase and Monsoon Disturbance Activity

In order to quantify changes in monsoon disturbance frequency (MDF) associated with MJO phase, we present contour plots of basic state MDF (Figures 2a and 3a) as well as MJO-related perturbations to MDF for extended boreal winter and summer seasons (Figures 2b–2e and 3b–3e). For these figures we define MDF as the number of observed 6-hourly track positions per day for a 10° by 10° bin. During boreal summer, there are two main regions of monsoon disturbance activity: (1) a band along 20°N extending almost one-quarter of the way around the world from India into the western Pacific and (2) a region of high MDF just southwest of Central America (Figure 2a). Each of these regions of high MDF are centered in the northwest portion of an

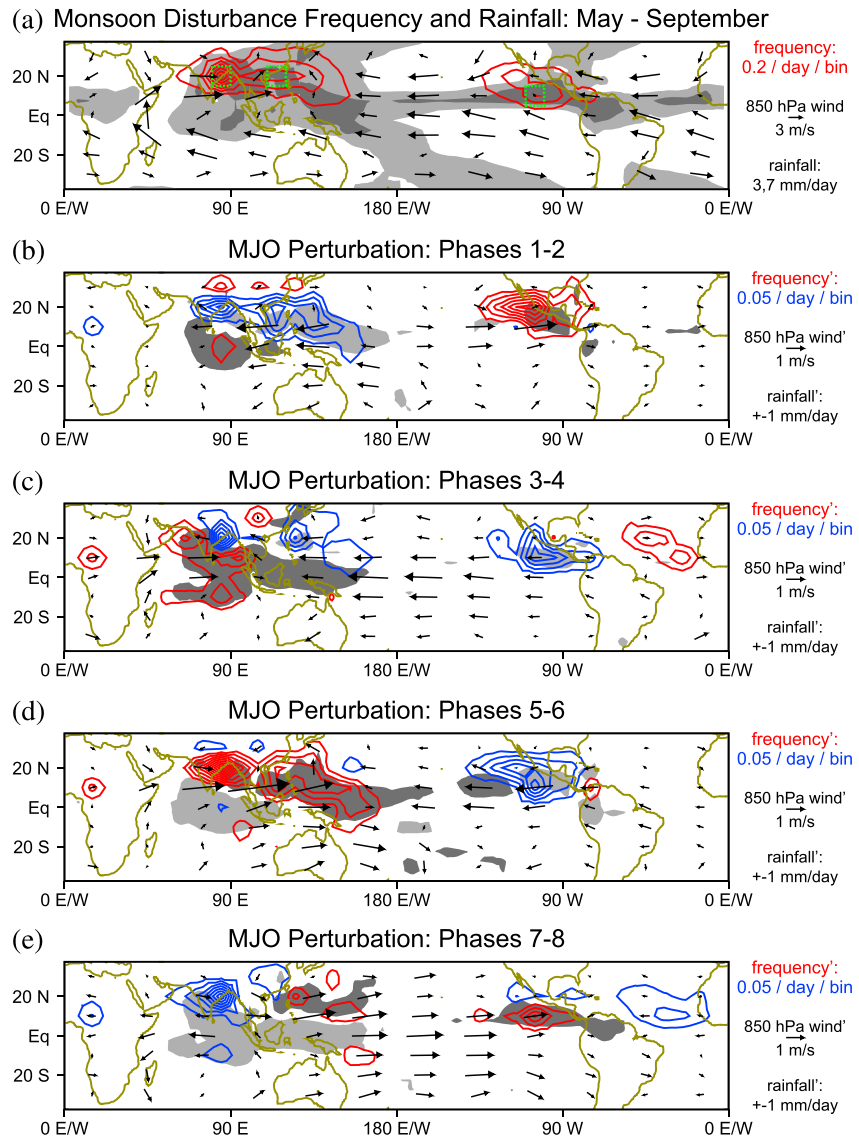


Figure 2. Monsoon disturbance frequency (MDF; colored contours), rainfall (gray shading), and 850 hPa winds (vectors) for May–September. (a) Seasonal mean values. (b–e) Deviations from local seasonal mean by MJO phase. Green boxes in Figure 2a outline regions with time evolution examined in more detail in Figure 4. In Figures 2b–2e, dark (light) shading denotes rainfall perturbations $>1 \text{ mm d}^{-1}$ ($< -1 \text{ mm d}^{-1}$). Red (blue) contours denote positive (negative) perturbations.

area of heavy rainfall (Figure 2a). During phases 1–2 of the boreal summer MJO, rainfall is enhanced over the central equatorial Indian Ocean and near the southern edge of central America and suppressed from central India into the western Pacific (Figure 2b). In these same regions there are perturbations to MDF of the same sign, although away from the equator, MDF perturbations are centered just west and north of the strongest rainfall perturbations. During phases 3 and 4, positive rainfall perturbations spread eastward and poleward from the Indian Ocean, and the sign of the rainfall perturbation near Central America reverses (Figure 2c). At this time, MDF is enhanced in much of the Indian Ocean but remains suppressed in eastern India. The MDF perturbation near Central America has also changed sign, following the behavior of the rainfall perturbation there. During phases 5 and 6, both rainfall and MDF perturbations are of opposite sign to those in phases 1 and 2 in most of the tropics (Figure 2d). The positive MDF perturbations near the Indian coast along the Bay of Bengal and in the West Pacific are especially strong (Figure 2d), rivaled only by those near Central America during phases 1 and 2, in strength and areal coverage (Figure 2b). During phases 7 and 8 negative

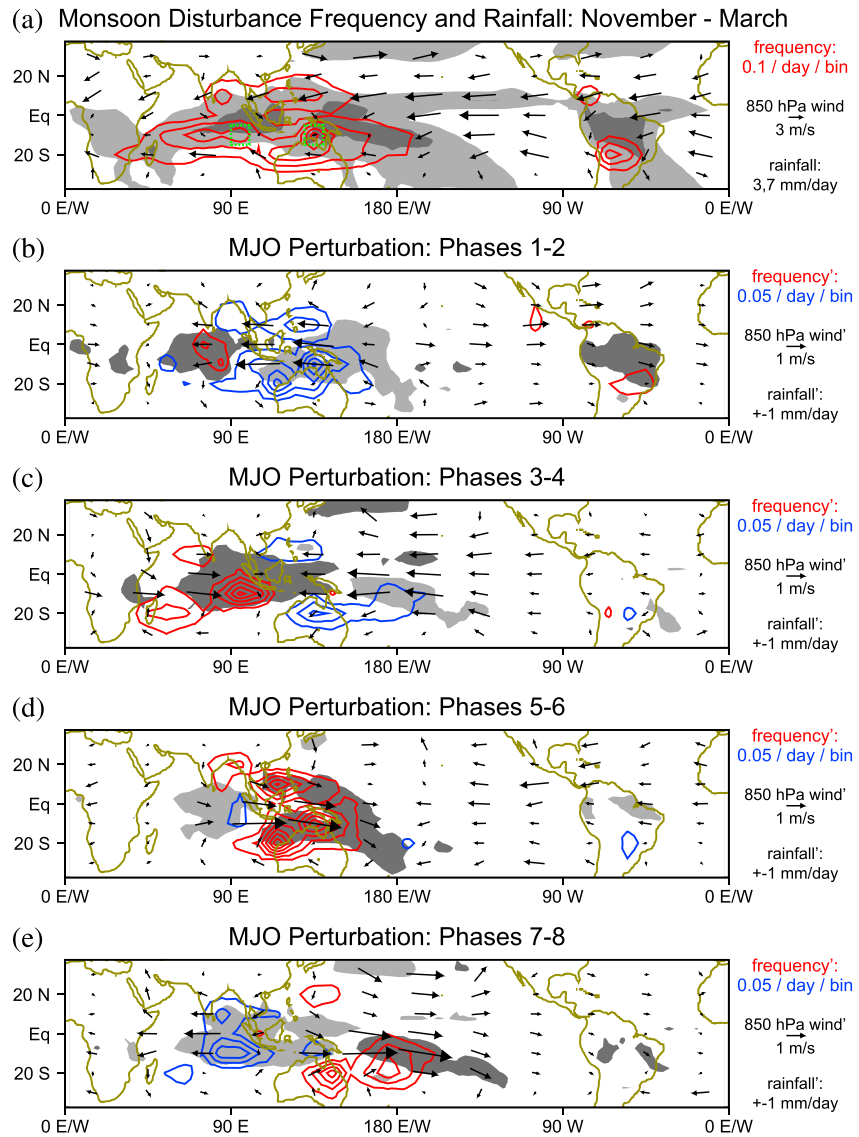


Figure 3. (a–e) Monsoon disturbance frequency, rainfall, and 850 hPa winds for November–March, contoured and shaded as in Figure 2.

rainfall perturbations cover much of the Indian Ocean and equatorial West Pacific, which are accompanied by negative MDF perturbations near India and across the equator from India (Figure 2e). A positive rainfall perturbation is collocated with a positive MDF perturbation in the East Pacific Intertropical Convergence Zone (ITCZ) at this time.

In boreal winter, monsoon disturbance activity is concentrated along the northern and southern edges of a region of heavy rainfall that extends from the central Indian Ocean through the South Pacific Convergence Zone (SPCZ; Figure 3a). Smaller regions of enhanced MDF occur poleward of the region of heavy rainfall over South America (Figure 3a). During phases 1 and 2 of the MJO, positive MDF and rainfall perturbations lie over the central Indian ocean, and negative MDF and rainfall perturbations extend from northwest Australia into the western Pacific (Figure 3b). Over time, the positive rainfall perturbation in the Indian Ocean expands and spreads eastward across the maritime continent and then southeastward over the SPCZ (Figures 3c–3e). Throughout this time positive MDF perturbations occur along the poleward and western flanks of this rainfall perturbation (Figures 3c–3e). Variations in MDF over South America are much weaker and more localized than those over the Indian and western Pacific Oceans (Figures 3b–3e).

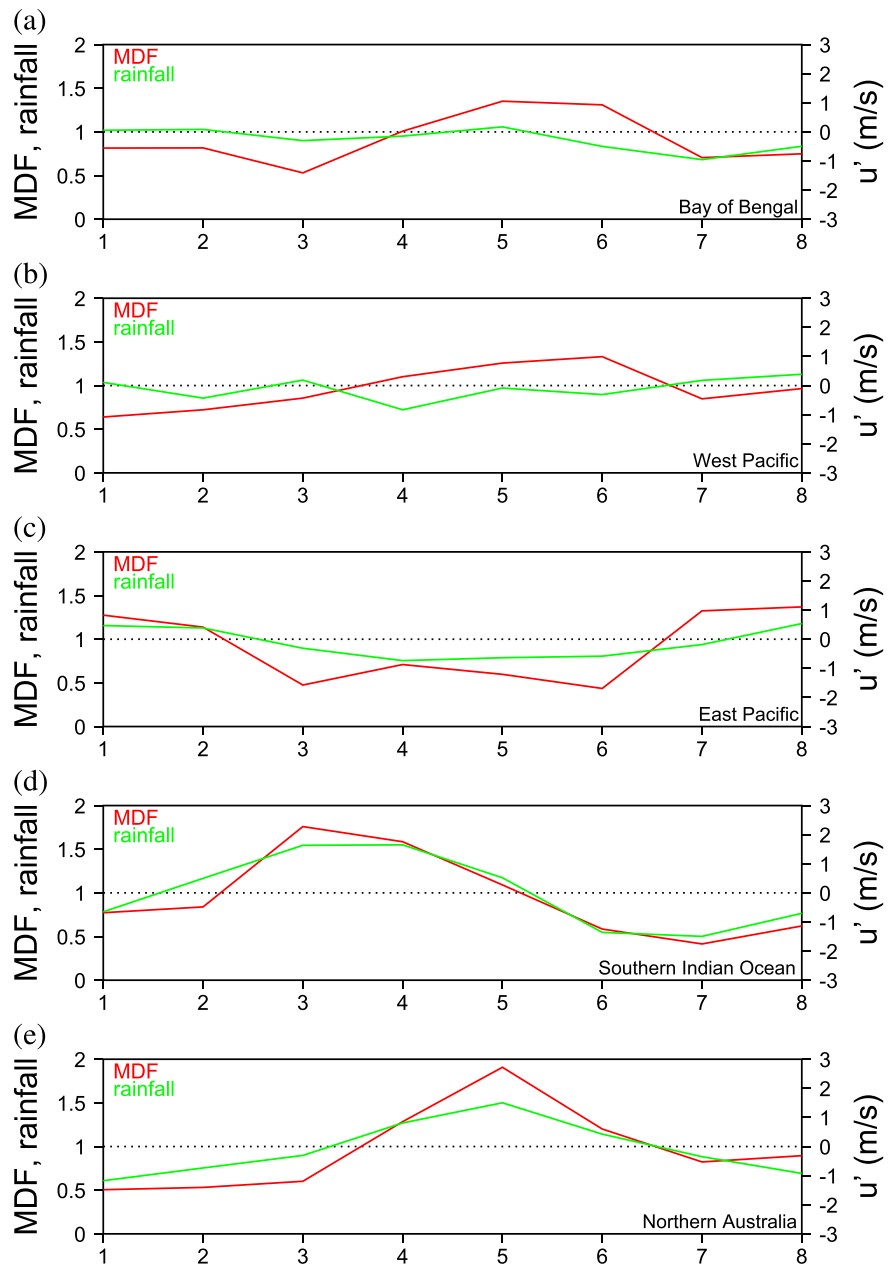


Figure 4. MJO phase dependence of monsoon disturbance frequency (MDF; red) and rainfall (green) for regions outlined in green in Figures 2a and 3a. (a) Bay of Bengal (80–90°E, 15–25 N). (b) West Pacific (110–120°E, 15–25 N). (c) East Pacific (250–260°E, 5–15 N). (d) South Indian Ocean (90–100°E, 5–15 S). (e) Australia Coast (130–140°E, 5–15 S). MDF and rainfall are normalized by dividing by seasonal mean values.

Figure 4 shows variations in MDF (red) over the phases of the MJO for the locations with the highest monsoon disturbance activity, which are outlined with dashed green boxes in Figures 2a and 3a. The MDF curves in Figure 4 are normalized by dividing by local seasonal mean values, so it is easy to discern the relative amplitude of perturbations associated with the MJO. Near the Indian coast along the Bay of Bengal, the amplitude of MJO-related perturbations to MDF approaches one-half of the seasonal mean value, with the minimum occurring in phase 3 and the highest values in phases 5 and 6 (Figure 4a). Over the West Pacific, MJO-related MDF perturbations are slightly weaker, with similar phasing (Figure 4b). In the East Pacific, the MDF maximum occurs in phase 8, with low MDF in phases 3–6 (Figure 4c). Local MDF perturbations associated with the MJO are especially strong in boreal winter in the Southern Hemisphere (Figures 4d and 4e). In the southern Indian

Ocean positive MDF perturbations reach 76% of the seasonal mean value during phase 3 (Figure 4d), and near the northern Australian coast positive MDF perturbations reach 90% of the seasonal mean value during phase 5 (Figure 4e). Negative MDF perturbations are slightly weaker but occur over more MJO phases than the positive ones in these regions. In other words, the MJO rainy period is accompanied by a local spike in MDF (Figures 4d and 4e). We conclude that monsoon disturbance activity varies strongly with MJO phase across the tropics.

4. How Does the MJO Modulate Monsoon Disturbances?

There is no scientific consensus on the fundamental dynamics of monsoon disturbances. Baroclinic instability was for years commonly cited as the growth mechanism of Indian monsoon depressions [Shukla, 1978; Mak, 1983; Moorthi and Arakawa, 1985; Krishnakumar et al., 1992; Krishnamurti et al., 2013]. However, Cohen and Boos [2016] showed that the potential vorticity structures of Indian monsoon depressions do not satisfy a necessary criterion for baroclinic instability. Monsoon depressions seem to have dynamical structures and climatological sensitivities to environmental parameters similar to those of weak tropical cyclones [Cohen and Boos, 2016; Ditchek et al., 2016], which supports the idea that at least some monsoon depressions are simply tropical depressions whose further intensification is inhibited by the strong vertical wind shear of monsoons. As it does for tropical cyclone frequency, the MJO might thus enhance MDF by creating a moist, vorticity-rich environment [Camargo et al., 2009]. East Pacific monsoon disturbances (or easterly waves) have been shown to extract energy from the barotropic shear of the time mean state and are influenced by horizontal moisture gradients, with more favorable conditions for development occurring in the westerly phase of the MJO [Crosbie and Serra, 2014; Rydbeck and Maloney, 2014, 2015].

These studies motivate a close look at how MDF perturbations relate to the MJO's low level to midlevel wind and moisture perturbations (Figure 5). Away from the equator, maxima in MDF typically occur in or near the western edge of positive midlevel moisture anomalies, in regions where the MJO's equatorial low level westerlies enhance cyclonic shear. Such maxima occur in local summer seasons to the west of Central America in phase 1 (Figure 5a), over eastern India in phase 5 (Figure 5b), east of Madagascar in phase 3 (Figure 5c), and west of Australia in phase 5 (Figure 5d). Near and on the equator, MDF is typically enhanced within the highest amplitude moisture anomalies, which often lie just to the east of the strongest westerlies. Examples of this kind of MDF enhancement occur in the boreal summer in the equatorial western Pacific in phase 5 (Figure 5b) and in austral summer in the eastern Indian Ocean in phase 3 (Figure 5c) and just north of Australia in phase 5 (Figure 5d).

These results suggest that different mechanisms are operating in near-equatorial and off-equatorial locations. Away from the equator, monsoon disturbance genesis and growth is apparently fostered by a combination of enhanced midlevel moisture and low level cyclonic vorticity, which might operate via barotropic amplification in some regions [Crosbie and Serra, 2014; Rydbeck and Maloney, 2014] or via a tropical cyclone genesis route in others [Hendricks et al., 2004; Cohen and Boos, 2016]. In contrast, near and on the equator MDF, rainfall and moisture are enhanced simultaneously (Figures 4c–4e), in regions where there is low level zonal wind convergence (Figure 5), which implies large-scale upward motion. Presumably, convective systems of all types are enhanced in these locations.

Previous studies have examined how the MJO modulates the genesis of tropical cyclones, with findings consistent with those presented here. In particular, tropical storm genesis was found to be 2–5 times more likely during the convectively active phase of the MJO than during the convectively suppressed phase for the Indian Ocean and West Pacific [Liebmann et al., 1994], Australia [Hall et al., 2001], East Pacific [Maloney and Hartmann, 2001], and South Indian Ocean [Bessafi and Wheeler, 2006; Duvel, 2015]. Similar ratios for monsoon disturbance genesis frequencies between MJO active and suppressed phases are shown in Figure 4. Moreover, previous studies also noted enhanced tropical storm genesis in the region just poleward of MJO westerlies, where there is a low level cyclonic vorticity perturbation, and in some cases reduced vertical wind shear [Hall et al., 2001; Bessafi and Wheeler, 2006; Duvel, 2015], which is also similar to our results for monsoon disturbances as depicted in Figure 5. One reason to expect the MJO to modulate monsoon disturbances in a similar way to tropical cyclones is that most of the increase in tropical storms during the MJO's convectively active phase is attributable to an increase in the tropical depressions from which the storms form [Liebmann et al., 1994; Duvel, 2015].

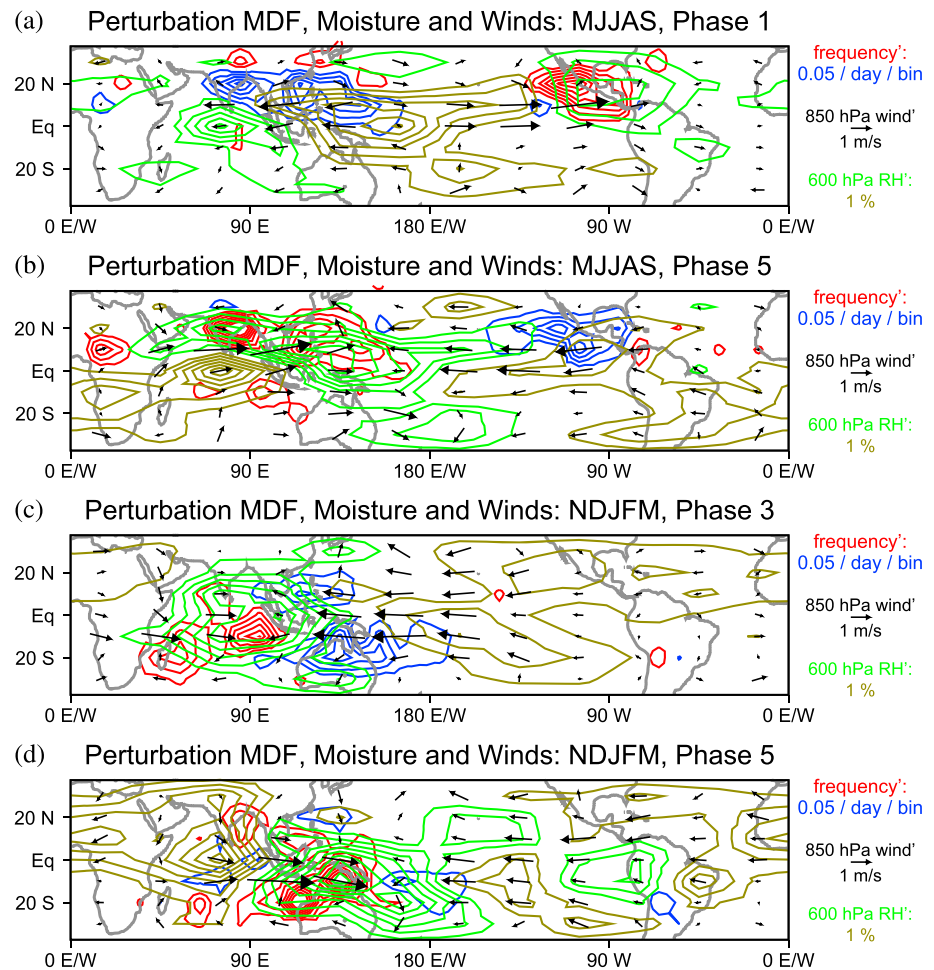


Figure 5. Monsoon disturbance frequency (red/blue), 600 hPa moisture (green/gold), and 850 hPa wind perturbations for May–September MJO phases (a) 1 and (b) 5 and November–March MJO phases (c) 3 and (d) 5. Green (gold) contours denote positive (negative) moisture perturbations.

One aspect of the MJO's modulation of monsoon disturbances that is difficult to quantify is its indirect, multi-scale impact. It is well known that the MJO comprises a hierarchy of convective systems, with various periods and scales, with some propagating eastward and some propagating westward [Nakazawa, 1988; Liebmann et al., 1994; Chen et al., 1996; Nasuno et al., 2009]. Some of the convective systems spawned by the MJO could create synoptic-scale wind circulations favorable for monsoon disturbance development [Straub and Kiladis, 2003; Kiladis et al., 2009] and/or local moisture and temperature anomalies that make spin-up more likely owing to impacts on the vertical structure of convective heating [Raymond and Sessions, 2007]. Note that such multiscale effects would not necessarily show up in MJO filtering, because waves embedded in the MJO often have positive and negative phases that cancel out when averaging is done over long time and spatial scales [Haertel and Kiladis, 2004; Nasuno et al., 2009]. Therefore, a careful assessment of these multiscale effects would require the tracking and counting of the various kinds of convective systems that the MJO comprises [Chen et al., 1996; Duvel, 2015] and relating their locations to those of monsoon disturbances.

5. Summary

There are several key results from this work. First, we show that the spatial climatology of monsoon disturbances is largely insensitive to the amplitude of the MJO. Second, we establish that the local, temporal modulation of monsoon disturbances by the MJO discussed in a number of previous studies is a global phenomenon. Finally, we describe a globally consistent pattern of how the MJO's modulation of monsoon disturbance frequency (MDF) relates to local wind and moisture perturbations. Away from the equator,

there are more monsoon disturbances in regions where the MJO's equatorial westerlies enhance cyclonic shear, near the western edge of midlevel moisture anomalies. Near and on the equator, MDF is enhanced in regions of zonal wind convergence where midlevel moisture and rainfall are enhanced. Further work is needed to fully explain the mechanism(s) of interaction between the MJO and monsoon disturbances, but our results are consistent with previous arguments for the growth of monsoon disturbances in moist and/or vorticity-rich environments [Ditchek et al., 2016; Rydbeck and Maloney, 2015; Prajeesh et al., 2013].

Acknowledgments

The monsoon depression data set used for this study is available at <http://earth.geology.yale.edu/depressdata>. This research was supported by ONR grant N00014-15-1-2531, by NSF grants AGS-1116885, AGS-125322, and AGS-1561066, and by the Yale Center for Research Computing.

References

- Berry, G. J., M. J. Reeder, and C. Jakob (2012), Coherent synoptic disturbances in the Australian monsoon, *J. Clim.*, *25*(24), 8409–8421, doi:10.1175/JCLI-D-12-00143.1.
- Bessafi, M., and M. C. Wheeler (2006), Modulation of south Indian Ocean tropical cyclones by the Madden-Julian Oscillation and convectively-coupled equatorial waves, *Mon. Wea. Rev.*, *134*, 638–656.
- Chen, S. S., R. A. Houze Jr., and B. E. Mapes (1996), Multiscale variability of deep convection in relation to large-scale circulation in TOGA COARE, *J. Atmos. Sci.*, *53*(10), 1380–1409.
- Chen, T.-C., and S.-P. Weng (1999), Interannual and intraseasonal variations in monsoon depressions and their westward-propagating predecessors, *Mon. Weather Rev.*, *127*(6), 1005–1020, doi:10.1175/1520-0493(1999)127<1005:IAIVIM>2.0.CO;2.
- Camargo, S. J., M. C. Wheeler, and A. H. Sobel (2009), Diagnosis of the MJO modulation of tropical cyclogenesis using an empirical index, *J. Atmos. Sci.*, *66*, 3061–3074, doi:10.1175/2009JAS3101.1.
- Cohen, N. Y., and W. R. Boos (2016), Perspectives on moist baroclinic instability: Implications for the growth of monsoon depressions, *J. Atmos. Sci.*, *73*, 1767–1788.
- Crosbie, E., and Y. Serra (2014), Intraseasonal modulation of synoptic-scale disturbances and tropical cyclone genesis in the eastern North Pacific, *J. Clim.*, *27*, 5724–5745.
- Davidson, N. E., and G. J. Holland (1987), A diagnostic analysis of two intense monsoon depressions over Australia, *Mon. Weather Rev.*, *115*, 380–392.
- Dee, D. P., et al. (2011), The ERA-Interim reanalysis: Configuration and performance of the data assimilation system, *Q. J. R. Meteorol. Soc.*, *137*, 553–597.
- Ditchek, S. D., W. R. Boos, S. J. Camargo, and M. K. Tippett (2016), A genesis index for monsoon disturbances, *J. Clim.*, *29*(14), 5189–5203.
- Duvel, J.-P. (2015), Initiation and intensification of tropical depressions over the Southern Indian Ocean: Influence of the MJO, *Mon. Weather Rev.*, *143*, 2170–2191.
- Fedorov, A. V., S. Hu, M. Lengaigne, and E. Guilyardi (2015), The impact of westerly wind bursts and ocean initial state on the development and diversity of El Niño events, *Clim. Dyn.*, *44*, 1381–1401.
- Goswami, B. N., R. S. Ajayamohan, P. K. Xavier, and D. Sengupta (2003), Clustering of synoptic activity by Indian summer monsoon intraseasonal oscillations, *Geophys. Res. Lett.*, *30*(8), 1431, doi:10.1029/2002GL016734.
- Haertel, P. T., and G. N. Kiladis (2004), Dynamics of 2-day equatorial waves, *J. Atmos. Sci.*, *61*(22), 2707–2721.
- Hall, J. D., A. J. Matthews, and D. J. Karoly (2001), The modulation of tropical cyclone activity in the Australian region by the Madden-Julian Oscillation, *Mon. Wea. Rev.*, *129*, 2970–2982.
- Hendricks, E. A., M. T. Montgomery, and C. A. Davis (2004), On the role of 'vortical' hot towers in formation of tropical cyclone Diana (1984), *J. Atmos. Sci.*, *61*, 1209–1232.
- Huffman, G. J., R. F. Adler, M. M. Morrissey, D. T. Bolvin, S. Curtis, R. Joyce, B. McGavock, and J. Susskind (2001), Global precipitation at one-degree daily resolution from multisatellite observations, *J. Hydrometeorol.*, *2*, 36–50.
- Hurley, J. V., and W. R. Boos (2015), A global climatology of monsoon low pressure systems, *Q. J. R. Meteorol. Soc.*, *141*, 1049–1064, doi:10.1002/qj.2447.
- Kiladis, G. N., K. H. Straub, and P. T. Haertel (2005), Zonal and vertical structure of the Madden-Julian Oscillation, *J. Atmos. Sci.*, *62*, 2790–2809.
- Kiladis, G. N., M. C. Wheeler, P. T. Haertel, K. H. Straub, and P. E. Roundy (2009), Convectively coupled equatorial waves, *Rev. Geophys.*, *47*, RG2003, doi:10.1029/2008RG000266.
- Krishnakumar, V., R. N. Keshavamurthy, and S. V. Kasture (1992), Moist baroclinic instability and the growth of monsoon depressions—Linear and nonlinear studies, *Proc. Indian Acad. Sci. - Earth Planet. Sci.*, *101*(2), 123–152, doi:10.1007/BF02840349.
- Krishnamurthy, V., and R. S. Ajayamohan (2010), Composite structure of monsoon low pressure systems and its relation to Indian rainfall, *J. Clim.*, *23*, 4285–4305.
- Krishnamurti, T. N., A. Martin, R. Krishnamurti, A. Simon, A. Thomas, and V. Kumar (2013), Impacts of enhanced CCN on the organization of convection and recent reduced counts of monsoon depressions, *Clim. Dyn.*, *41*(1), 117–134, doi:10.1007/s00382-012-1638-z.
- Liebmann, B. L., H. H. Hendon, and J. D. Glick (1994), The relationship between tropical cyclones of the western Pacific and Indian Oceans and the Madden-Julian Oscillation, *J. Meteorol. Soc. Jpn.*, *72*, 401–412.
- Lorenz, D. J., and D. L. Hartmann (2006), The effect of the MJO on the North American Monsoon, *J. Clim.*, *19*, 333–343.
- Madden, R., and P. Julian (1971), Detection of a 40–50 day oscillation in the zonal wind in the tropical Pacific, *J. Atmos. Sci.*, *70*(2), 702–708.
- Madden, R., and P. Julian (1972), Description of global-scale circulation cells in the tropics with a 40–50 day period, *J. Atmos. Sci.*, *29*, 1109–1123.
- Madden, R. A., and P. R. Julian (1994), Observations of the 40–50 day tropical oscillation—A review, *Mon. Weather Rev.*, *122*, 814–837.
- Mak, M. (1983), A moist baroclinic model for monsoonal mid-tropospheric cyclogenesis, *J. Atmos. Sci.*, *40*, 1154–1162.
- Maloney, E. D., and D. L. Hartmann (2000), Modulation of hurricane activity in the Gulf of Mexico by the Madden-Julian Oscillation, *Science*, *287*, 2002–2004.
- Maloney, E. D., and D. L. Hartmann (2001), Modulation of Eastern North Pacific hurricanes by the Madden-Julian Oscillation, *J. Clim.*, *13*, 1451–1460.
- Mooley D. A., and J. Shukla (1987), Characteristics of the westwardmoving summer monsoon low-pressure systems over the Indian region and their relationship with the monsoon rainfall, *Tech. Rep.*, 218 pp., Cent. for Ocean-Land-Atmos. Interact., Univ. of Md, College Park.
- Moorthi, S., and A. Arakawa (1985), Baroclinic instability with cumulus heating, *J. Atmos. Sci.*, *42*(19), 2007–2031.
- Nakazawa, T. (1988), Tropical super clusters within intraseasonal variations over the western Pacific, *J. Meteorol. Soc. Jpn.*, *66*(6), 823–839.
- Nasuno, T., H. Miura, M. Satoh, A. T. Noda, and K. Ouchi (2009), Multi-scale organization of convection in a global numerical simulation of the December 2006 MJO event using explicit moist processes, *J. Math. Soc. Jpn.*, *87*(2), 335–345.

- Prajeesh, A. G., K. Ashok, and D. V. B. Rao (2013), Falling monsoon depression frequency: A Gray-Sikka conditions perspective, *Sci. Rep.*, *3*, 2989, doi:10.1038/srep02989.
- Raymond, D. J., and S. L. Sessions (2007), Evolution of convection during tropical cyclogenesis, *Geophys. Res. Lett.*, *34*, L06811, doi:10.1029/2006GL028607.
- Rydbeck, A. V., and E. D. Maloney (2014), Energetics of East Pacific easterly waves during intraseasonal events, *J. Clim.*, *27*, 7603–7621.
- Rydbeck, A. V., and E. D. Maloney (2015), On the convective coupling and moisture organization of East Pacific easterly waves, *J. Atmos. Sci.*, *72*, 3850–3870.
- Shukla, J. (1978), CISK-barotropic-baroclinic instability and the growth of monsoon depressions, *J. Atmos. Sci.*, doi:10.1175/1520-0469(1978)035<0495:CBBIAT>2.0.CO;2.
- Sikka, D. R. (2006), A study on the monsoon low pressure systems over the Indian region and their relationship with drought and excess monsoon seasonal rainfall, Center for Ocean-Land-Atmosphere Studies, Center for the Application of Research on the Environment.
- Straub, K. H., and G. N. Kiladis (2003), Interactions between the boreal summer intraseasonal oscillation and higher-frequency tropical wave activity, *Mon. Weather Rev.*, *131*(5), 945–960.
- Wang, B., and H. Rui (1990), Synoptic climatology of transient tropical intraseasonal convection anomalies: 1975–1985, *Meteorol. Atmos. Phys.*, *44*, 43–61, doi:10.1007/BF01026810.
- Wheeler, M., and H. Hendon (2004), An all-season real-time multivariate MJO index: Development of an index for monitoring and prediction, *Mon. Weather Rev.*, *132*, 1917–1932.
- Wheeler, M., and G. N. Kiladis (1999), Convectively coupled equatorial waves: Analysis of clouds and temperature in the wavenumber-frequency domain, *J. Atmos. Sci.*, *56*, 374–399.
- Wu, M. L. C., S. Schubert, and N. E. Huang (1999), The development of the South Asian summer monsoon and the intraseasonal oscillation, *J. Clim.*, *12*, 2054–2075.
- Yasunari, T. (1981), Structure of an Indian summer monsoon system with around 40-day period, *J. Meteorol. Soc. Jpn.*, 336–354.
- Zhang, C. (2005), Madden Julian Oscillation, *Rev. Geophys.*, *43*, RG2003, doi:10.1029/2004RG000158.